Evapotranspiration Variations in the Mississippi River Basin Estimated From GPS Observations

Tengyu Zhang and Shuanggen Jin, *Member, IEEE*

***Abstract*—Evapotranspiration (ET) is one of the key variables in water cycle and ecological systems, whereas it is difficult to quantify ET variations from traditional observations in large river basins, e.g., Mississippi River basin (MRB). In this paper, a new geodetic tool, i.e., Global Positioning System (GPS), is used for the first time to estimate monthly ET variations at a regional scale. Based on the water balance equation, the monthly ET variation is estimated using the GPS-derived terrestrial water storage (TWS) from January 2006 to July 2015 in MRB. The annual amplitude of GPS-inferred TWS in MRB agrees well with the results of Gravity Recovery and Climate Experiment. The ET variations from the water balance approach agree well with the land surface modeling and remote sensing data. The correlation of GPS-inferred ET with other ET products is higher than 0.8, which indicates that the GPS-estimated ET well characterizes the ET variations in MRB. The annual amplitude of GPS-inferred ET variations is 47.9 mm/month, which is close to that from land surface modeling of North American Land Data Assimilation System, and a little larger than MODerate Resolution Imaging Spectroradiometer. The mean monthly ET reaches its maximum in June–July and its minimum in December, which is consistent with the periodic pattern of radiative energy in a year. Furthermore, the ET variations are mainly dominated by the temperature change in MRB.**

***Index Terms*—Evapotranspiration (ET), Global Positioning System (GPS), Gravity Recovery and Climate Experiment (GRACE), Mississippi River basin (MRB), terrestrial water storage (TWS).**

I. INTRODUCTION

THE Mississippi River basin (MRB) is one of the largest river basins in the world with about 3.2 million km^2, which is one of the most important ecological systems for the agricultural economy in the United States [1]. It is essential to monitor and understand the variability of water resources in MRB. Evapotranspiration (ET) plays a key role in controlling the water and energy balance in a region that is the highest outgoing water flux in the hydrological cycle. ET, including evaporation and transpiration from the land, contributes to replenish the atmospheric moisture with the process of precipitation recycling [2] and controls the hydrological cycle in the ecosystem. The determination of ET is very helpful for irrigation design and scheduling [3] and even provides some additional information for weather forecasting [4]. Therefore, characterization and quantification of ET in MRB have become more and more important.

The traditional approach for micrometeorological measurements cannot provide enough observations to monitor ET variations. Nowadays, satellite remote sensing can monitor the variability of ET at global and regional scales. The MODerate Resolution Imaging Spectroradiometer (MODIS) has become an essential tool to estimate the spatially distributed ET variations [5], [6]. Based on an empirical method [7] and physical models [8], two kinds of approaches have been developed to obtain ET products. Vegetation index-based data and land surface temperature are inputs to energy balance formulation, which showed some strengths and weaknesses [9]. It is necessary to calibrate the model results using ancillary data such as air temperature, wind speed, and surface resistance parameters at a specific region, which is the limitation for the method [10]. Another indirect method to estimate ET is based on the water balance equation [11] and the terrestrial water storage (TWS) change in the region of interest. Since the Gravity Recovery and Climate Experiment (GRACE) mission has been successfully launched in 2002, the monthly gravity field data have been obtained and widely used to estimate the large-scale mass change [12], including global and regional hydrological cycles [13], [14], and the ET variations at basin scale [15], [16]. The estimated monthly ET showed good consistency with the European Centre for Medium-Range Weather Forecasts reanalysis and the Global Land Data Assimilation System (GLDAS) models [17]. However, GRACE has large noises and low temporal–spatial resolutions, e.g., 300- to 500-km spatial resolutions.

Another important geodetic tool, i.e., Global Positioning System (GPS) measurement, is very sensitive to large-scale mass redistribution [18], which has a great potential to estimate regional TWS changes. Some attempts have been done to determine the surface loading change [19] and seasonal patterns [20], which demonstrated that GPS can be independent and efficient to monitor and quantify TWS change [20], [21]. GRACE has a limitation for its application at some small regional scale, whereas dense GPS observations are more sensitive to hydrological loads at the scale of kilometers to hundreds of

Manuscript received October 18, 2015; revised December 21, 2015 and March 14, 2016; accepted March 29, 2016. Date of publication April 20, 2016; date of current version June 1, 2016. This work was supported in part by the National Keystone Basic Research Program (MOST 973) under Grant 2012CB72000, by the Shanghai Science and Technology Commission Project under Grant 12DZ2273300, and by the National Natural Science Foundation of China Project under Grant 11373059. *(Corresponding author: Shuanggen Jin.)*

T. Zhang is with Shanghai Astronomical Observatory, Chinese Academy of Sciences, Shanghai 200030, China, and also with the University of Chinese Academy of Sciences, Beijing 100049, China.

S. Jin is with the Key Laboratory of Planetary Sciences, Shanghai Astronomical Observatory, Chinese Academy of Sciences, Shanghai 200030, China, and also with the Department of Geomatics Engineering, Bülent Ecevit University, Zonguldak 67100, Turkey (e-mail: sgjin@shao.ac.cn; sg.jin@yahoo.com).

Color versions of one or more of the figures in this paper are available online at http://ieeexplore.ieee.org.

Digital Object Identifier 10.1109/TGRS.2016.2549364

kilometers. Fu *et al.* [21] have successfully obtained the water loading distribution in Washington and Oregon at a small region. Therefore, continuous GPS observations with a low cost and a dense network can be an appropriate supplementary tool.

Moreover, it is really essential to understand the sensitivity of ET variations to soil moisture and temperature, which are two controlling factors in the coupled land–atmosphere system. It is a classic ecohydrological problem to distinguish the ET variations responding to the atmospheric demand from that of the terrestrial soil moisture at regional and local scales. Due to the complex ET-soil moisture coupling and ET-temperature coupling, it is difficult to uncouple the effect of soil moisture and temperature on ET variations. The ET variation depends on the surface and subsurface characteristics in response to the changing atmospheric demand, which has a strong correlation with surface temperature. On the other hand, with decreasing soil moisture content, the plant root will have less accessible moisture, which contributes to reduced ET. Therefore, the limited soil moisture supply will lead to restricted ET.

In this paper, we aim to estimate ET variations from continuous GPS observations in MRB and compare them with other models and remote sensing results. In Section II, the data are introduced as the basic input for estimation of ET variation. In Section III, the theory of GPS-estimated TWS and ET based on the water balance equation is presented. The results and comparison with other models and observations are presented in Section IV, as well as effects on ET variations. Finally, the conclusion is summarized in Section V.

II. Observation Data

A. GPS and GRACE Observations

Space geodetic observations can estimate surface water variations, e.g., GRACE and GPS. TWS includes all forms of water underneath and above the land surface, such as snow, surface water, soil moisture, and groundwater. The seasonal variations of hydrological loading in a regional region, e.g., lake [19], [22] and river basin [23], have been studied by GPS measurements. The continuous GPS observations at 350 stations with almost 20 years provide unique data to estimate hydrological loading change in MRB (see Fig. 1), which covers from 30° N to 50° N and 78° W to 114° W. The continuous GPS coordinate time series at precision of millimeters are obtained from the daily solutions of the Jet Propulsion Laboratory (JPL) processed by GIPSY software. To estimate water storage variations, the atmosphere loading should be removed from the GPS height time series first. Here, we remove the atmosphere effects using the data of 2.5° × 2.5° from the National Centers for Environmental Prediction. The atmosphere displacements are averaged into the daily value as a postprocessed correction for the GPS daily solution. The amplitude of the displacement caused by atmosphere loading is usually smaller when compared with hydrological loading [24].

Here, we used a continuous GPS coordinate time series from January 2006 to July 2015 to estimate TWS change. The daily time series have been filtered into monthly data to be consistent with precipitation data and GRACE data.

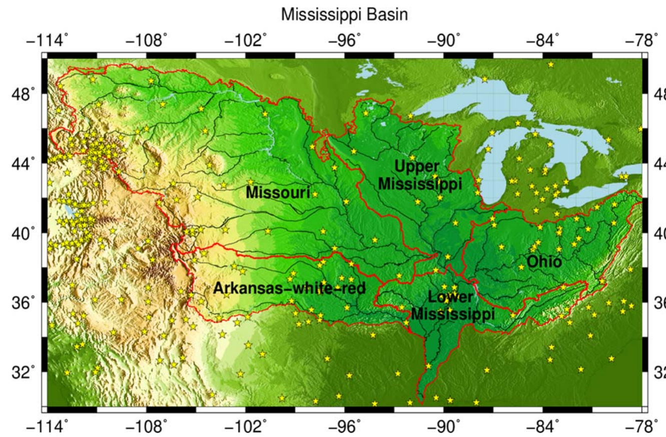

Fig. 1. Distribution of continuous GPS stations (yellow stars) in the region of MRB.

The method to invert TWS change will be introduced in the next section. The GRACE mission with more than ten years of observations provides a unique opportunity to estimate global mass redistribution within the Earth system. Here, we employed the level-2 monthly spherical harmonic coefficients of GRACE Release 05 from the Center for Space Research (CSR) of The University of Texas at Austin with a truncation degree of up to 60. The monthly gravity coefficients are provided by CSR (ftp://podaac-ftp.jpl.nasa.gov/allData/grace/L2/CSR/RL05/), which are used to obtain the TWS change from April 2006 to July 2015 for comparison with GPS results.

B. Precipitation and Runoff Data

The precipitation data are vital to the basin-scale ET estimation because it is the only input in the land storage. For the global scale, the rain gauge networks are installed to provide the measurement of precipitation, but it is far from assessing the regional precipitation. The monthly estimates of precipitation in MRB can be obtained from Parameter–elevation Regressions on Independent Slopes Model (PRISM) data, which were derived by the climate research initiative of Oregon State University known as the PRISM Climate Group [25]. The PRISM uses the point data, the digital elevation model, and other spatial data sets to generate gridded estimates of climatic parameters [26]. A wide range of observation networks has been gathered and specific quality control measurements have been applied to obtain short- and long-term climate patterns. The precipitation data from PRISM have been validated by *in situ* ground-based meteorological observations at reference stations [27]. PRISM provides the gridded precipitation data and surface temperature at a spatial resolution of 4 km from 1981 to 2015 (e.g., Fig. 2). Another precipitation data retrieved from the Tropical Rainfall Measurement Mission (TRMM) provide precipitation products from low to middle latitudes. The three hourly products from TRMM with a spatial resolution of 0.25° × 0.25° are converted into monthly solutions. These precipitation products are very close to each other with a high correlation of 0.98 (see Fig. 3).

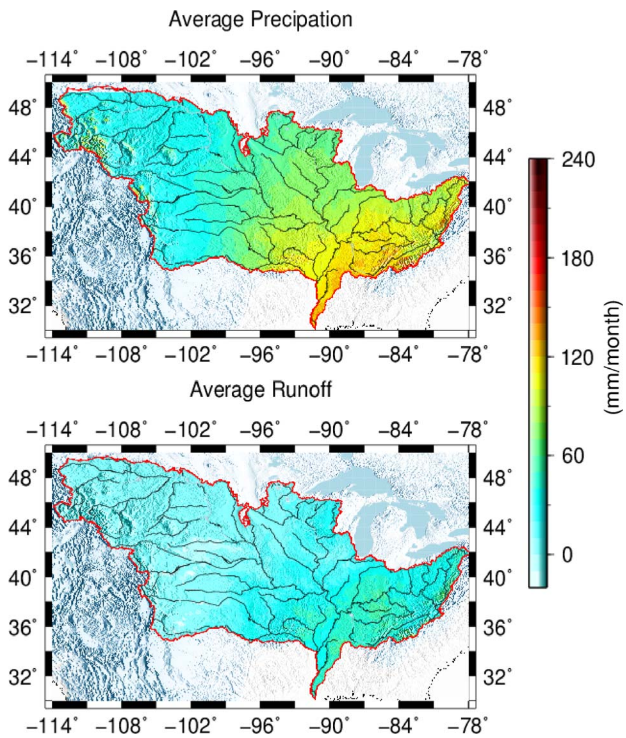

Fig. 2. Distribution of average precipitation from PRISM and average runoff from VIC.

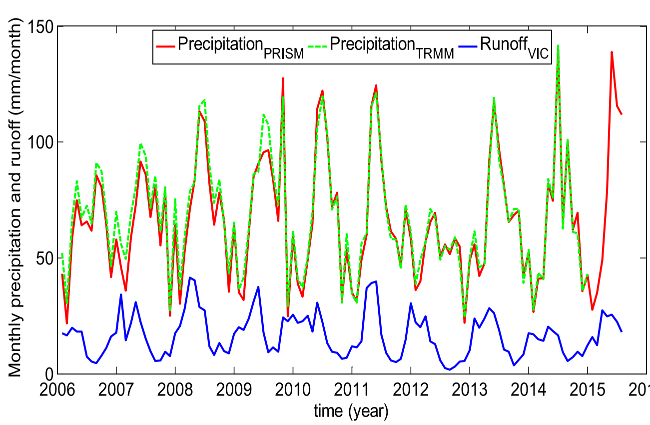

Fig. 3. Monthly time series of average precipitation and runoff over MRB from 2006 to July 2015.

The runoff of a river has been widely observed with sufficient accuracy, but the possibility to divulge information on the water usage leads to the unavailability of the observation data. The U.S. Army Corps of Engineers have dense gauge stations for the MRB, but the runoff data are unavailable in this study. The runoff data used in this paper are obtained from the North American Land Data Assimilation System (NLDAS) Variable Infiltration Capacity (VIC) model, which provides monthly runoff data at a spatial resolution of 12 km covering the whole United States. The model runoff has been validated by the stream flow of all the basins in the conterminous United States observed by the U.S. Geological Survey [28]. After the calibration [29], the VIC simulation parameters were improved for estimation of more reasonable runoff data. The spatially distributed average precipitation and runoff are derived from the released data, which show lower precipitation and runoff in the MRB and Ohio basin but larger in the whole region (see Fig. 2). The monthly precipitation and runoff time series have similar periodic pattern, but the amplitude of precipitation is larger than that of runoff (see Fig. 3).

C. *ET From Models and Remote Sensing Data*

The ET from NLDAS [28] and GLDAS [17] is used for comparison with our results. Using three different land surface models (LSMs), namely, Noah, Mosaic, and VIC as inputs, it will generate different models consisting of ET and soil moisture. The NLDAS and GLDAS models provide the products from 1979 to present, which specify values at 1/8° and 1° intervals of latitude and longitude, respectively. The NLDAS models assimilate observation data of North America, which provide simulation products in the United States (125° to 67° W, 25° to 53° N). The products from GLDAS cover globally from 60° S to 90° N, 180° W to 180° E. The ET products from MODIS are derived from MODIS-based phonological and surface variables and obtained from 2006 to 2015 (http://www.ntsg.umt.edu/project/mod16#data-product). The gridded ET products from MODIS with a spatial resolution of 1/20° are used for the comparison.

III. Theory and Methods

A. *TWS Estimation From GPS*

The Earth's crust will induce elastic displacements due to the surface mass loading underlying the solid Earth. The surface displacement can be accurately measured by GPS in millimeter-level accuracy. The well-known Green's functions [30] can be used to calculate the surface displacement in elastic response to the load of water, snow, ice, and atmosphere. The mass load is related to the vertical elastic displacements. Therefore, the vertical displacements are used to determine the distribution of the surface load. The elastic displacement can be expressed by the integration of the mass load and Green's function [18] as follows:

$$u(\theta) = \frac{\Delta M \times R}{M_e} \sum_{n=0}^{\infty} h_n P_n(\cos\theta) \tag{1}$$

where h_n is the elastic Love number, θ is the angular distance, P_n are the Legendre polynomials, R and M_e are the radius and mass of the Earth, and ΔM is the disk mass load. The load Love number is truncated up to degree 500 for the computation of the displacement. Therefore, TWS change can be estimated from the vertical displacement measured by GPS [21]. The regularization method and tradeoff method are applied during the inversion of TWS change. The details about the method can be found in [21].

B. TWS Estimation From GRACE

Here, we employed the level-2 monthly spherical harmonic coefficients from the CSR GRACE Release 05 with a truncation degree of up to 60. The processing strategy includes decorrelation destriping, smoothing, and filtering [32]. The C_{20} was usually replaced by the results from Satellite Laser Ranging data [33]. Some missing month data are interpolated from the adjacent two months. The residual Stokes coefficients are obtained after removing the mean gravity field for 2006–2015. To be consistent with the GPS processing strategy, the equivalent water thickness is determined by the approach in [34] without considering the atmosphere loading effects. Because the postprocessing of GRACE observations results in the leakage errors in TWS estimation with the omission of high-degree spherical harmonic coefficients [35], [36], the land-grid-scaling method is applied in this paper to restore the attenuating signal [34].

C. Water Balance Equation

The movement of all water above, on, and below the Earth's surface results in the hydrological cycle. The principle of mass conservation is the basic law in the hydrological cycle. The inflow, outflow, and water storage change in a region will be controlled by a simple rule. The flow of water in and out of a basin can be described by the water balance equation based on the conservation of mass in a closed system. The terrestrial water budget in basin scale can be expressed by the water balance equation as follows:

$$\mathrm{ET} = P - R - \partial S/\partial t \tag{2}$$

where ET is the evapotranspiration, P is the precipitation, R is the total basin discharge, and $\partial S/\partial t$ is the total water storage change averaged over space. Here, ∂t represents the sampling rate, which is one month consistent with the time resolution of data and models. Because precipitation and runoff data are the accumulation value in one month, $\partial S/\partial t$ should be calculated from the TWS change in two months of GRACE measurements. The details to derive the ET variations from TWS change were discussed by Rodell *et al.* [17].

The precipitation data can be obtained from the PRISM group with one-month interval. The simulated runoff data from the VIC model are used, which have good spatial distribution and accuracy [28]. The TWS changes in the MRB are estimated by continuous GPS measurements, which are the first attempt to be used for assessing the ET variations in MRB. This is a very straightforward method to estimate the monthly ET variations based on the water balance equation [31].

IV. Results and Discussion

A. TWS Variations From GPS, GRACE, and GLDAS

In order to confirm GPS-inferred TWS variations, the GRACE-estimated results are used for comparison (see Fig. 4). The monthly GPS TWS time series are filtered to attenuate the high-frequency noise. First, the seasonal water storage variation is derived from GPS measurements using the method proposed by Argus *et al.* [20] and the similar fitting method is employed for GRACE-derived TWS. The correlation of annual amplitude from GPS-inferred and GRACE-inferred TWS is 0.8. The distribution of annual amplitudes from GPS-inferred and GRACE-inferred TWS has a similar pattern (see Fig. 5). The west parts of Missouri, South MRB, and Ohio basin have slightly larger amplitude, but the central MRB from the GPS-inferred TWS has the largest amplitude, which is consistent with their physiographic coverage. On the other hand, GPS is more sensitive to surface water mass variations in smaller scale. Therefore, the seasonal amplitude of GPS-inferred TWS is larger than GRACE-inferred TWS.

Furthermore, the gridded GPS TWS variations are obtained from January 2006 to July 2015, which are compared with GRACE results. GLDAS-VIC monthly TWS data are also

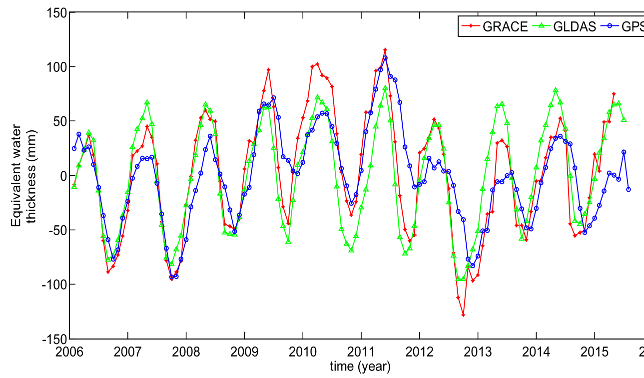

Fig. 4. Monthly time series of TWS from GRACE, GLDAS, and GPS for January 2006–July 2015.

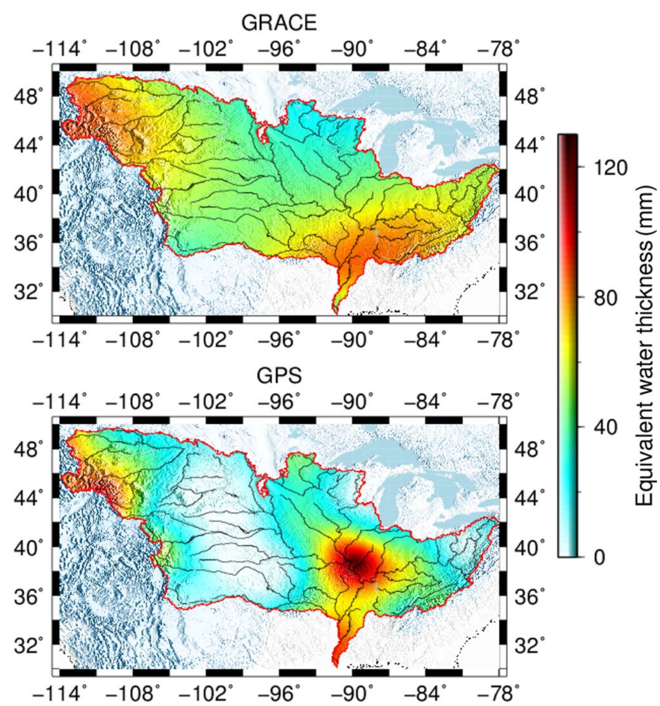

Fig. 5. Amplitudes of annual TWS variations from GRACE and GPS in MRB.

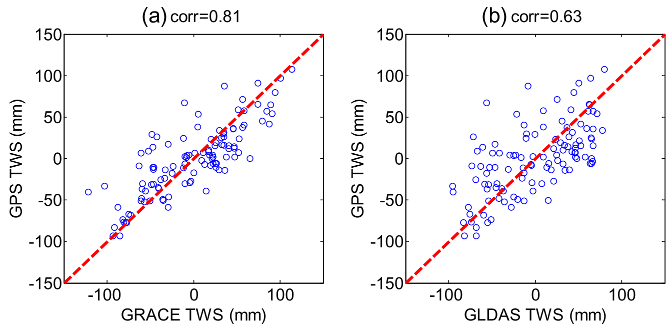

Fig. 6. (a) Scatter plot of GRACE-inferred TWS and GPS-inferred TWS. (b) Scatter plot of GLDAS TWS and GPS-inferred TWS.

obtained for comparison. GLDAS model is used to calibrate GRACE-derived TWS due to the signal attenuation and leakage errors [34]. Since the groundwater and surface water are not explicitly simulated in GLDAS models, they are not included in TWS [14]. GLDAS provides gridded data with a spatial resolution of $1^\circ \times 1^\circ$. Here, we use monthly GLDAS data from January 2006 to July 2015 to compare with GPS-inferred TWS. The GPS-inferred TWS change clearly shows similar seasonal patterns with GRACE-inferred TWS and GLDAS data, but GPS-inferred TWS time series have some high-frequency signals [37].

GPS and GRACE have relatively low TWS variations at the end of 2012 and early 2013, which indicate the dry period in MRB. GLDAS shows good consistency with GRACE TWS results. The correlation between GLDAS and GRACE is as high as 0.88. In order to validate the GPS-inferred TWS, Fig. 6 shows the scatter plot of monthly GRACE-TWS time series and GPS-TWS time series, as well as GLDAS-TWS and GPS-TWS. The correlation between GRACE-inferred TWS and GPS-inferred TWS is 0.81, whereas GLDAS has a low correlation of 0.63 with GPS-inferred TWS.

B. *ET Variations in MRB*

The gridded precipitation data from PRISM and runoff data from NLDAS are averaged into monthly time series. The ET change in MRB can be obtained by using the water balance equation method with a monthly TWS change. We use the GPS-inferred TWS to analyze the ET changes in MRB from 2006 to July 2015, which are compared with the GRACE results [15], [17]. The ET products from the LSM and remote sensing data are also obtained for comparison (see Fig. 7). All these ET products from different LSMs have good characterization of ET [38].

In order to evaluate these ET products, the mean value of these ET variations is subtracted from their time series. Fig. 7 shows the time series of monthly ET variations from the water budget approach, LSM simulations, and remote sensing analysis. Our estimated ET products are consistent with the results derived by Rodell *et al.* [39] in MRB. The ET products from the LSM are highly correlated with each other, and all of them have similar annual amplitudes and phases. In order to validate the consistency of GPS-derived ET with other ET products, Fig. 8 provides the scatter plot of monthly GPS-inferred

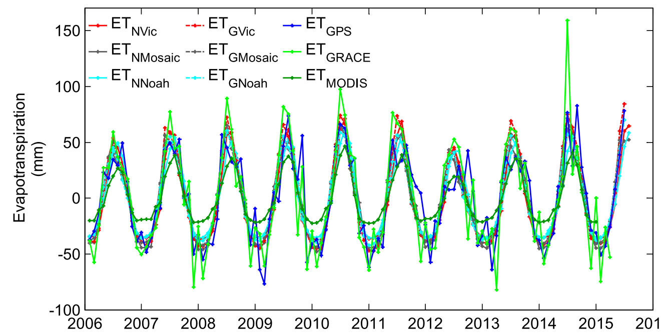

Fig. 7. Time series of monthly ET from LSMs (VIC, Mosaic, and Noah). NVic, NMosaic, and Nnoah are from NLDAS; GVic, Gmosaic, and GNoah are from GLDAS. The rest are from GPS, GRACE, and MODIS, respectively.

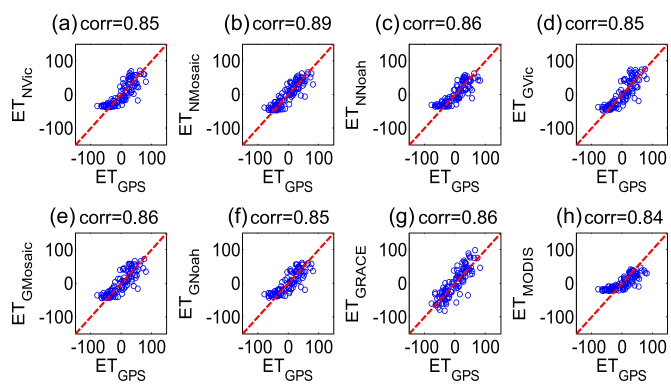

Fig. 8. Scatter plot of GPS-estimated ET with (a) NLDAS-VIC ET, (b) NLDAS Mosaic ET, (c) NLDAS Noah ET, (d) GLDAS VIC ET, (e) GLDAS Mosaic ET, (f) GLDAS Noah, (g) GRACE ET, and (h) MODIS ET.

ET with other ET estimates. It can be concluded that the ET estimation from GPS TWS with the water budget approach can well characterize the ET variations in MRB, which are highly correlated with LSMs, GRACE, and remote sensing results. The highest correlation is 0.89 between GPS-inferred ET and NLDAS-Mosaic ET, and the lowest correlation is 0.84 between GPS ET and MODIS ET. The correlation coefficients between different ET products are listed in Table I. In order to decipher the response of ET variations to precipitation changes, the correlation of ET products with precipitation from PRISM is calculated in MRB (see Table I). Correlation coefficients of the monthly precipitation with GPS and GRACE ET variations are as high as 0.81 and 0.8, respectively. The mean correlation coefficients between monthly precipitations with NLDAS LSMs, GLDAS LSMs, and MODIS are 0.67, 0.72, and 0.65, which indicate that ET products from LSM are highly correlated with precipitation than remote sensing ET products. The correlation difference among these ET products is mainly from different inputs, algorithms, and assumptions. The stronger correlation between ET products and precipitation may result from that LSMs are more responsive to soil moisture and, consequently, to precipitation than remote sensing results [38].

Because of the same category from land surface modeling, ET products from NLDAS and GLDAS have similar magnitudes. However, the magnitude of ET products from MODIS

TABLE I
CORRELATION COEFFICIENTS OF TIME SERIES OF PRECIPITATION WITH DIFFERENT ET PRODUCTS

Variable	P	ET_1	ET_2	ET_3	ET_4	ET_5	ET_6	ET_7	ET_8	ET_9
P	1.00	0.65	0.75	0.63	0.72	0.73	0.72	0.80	0.65	0.81
ET_1		1.00	0.96	0.99	0.97	0.96	0.97	0.88	0.98	0.85
ET_2			1.00	0.95	0.97	0.98	0.98	0.90	0.94	0.89
ET_3				1.00	0.95	0.94	0.95	0.87	0.98	0.86
ET_4					1.00	0.99	1.00	0.90	0.95	0.85
ET_5						1.00	0.99	0.90	0.94	0.86
ET_6							1.00	0.90	0.96	0.85
ET_7								1.00	0.86	0.86
ET_8									1.00	0.84
ET_9										1.00

$ET_{1\text{-}9}$ are from NLDAS-VIC, NLDAS-MOSAIC, NLDAS-Noah, GLDAS-VIC, GLDAS-MOSAIC, GLDAS-Noah, GRACE, MODIS and GPS, respectively.

TABLE II
ANNUAL AND SEMIANNUAL TERMS OF ET PRODUCTS, DOY (DAY OF YEAR)

	Annual		Semi-Annual	
	Amplitude (mm)	Maximum DOY	Amplitude (mm)	Phase (degree)
$ET_{N\text{-}Vic}$	46	204.8	12	38
$ET_{N\text{-}Mosaic}$	48	200.8	4	322
$ET_{N\text{-}Noah}$	43	206.8	9	66
$ET_{G\text{-}Vic}$	52.6	197.1	11.9	3.9
$ET_{G\text{-}Mosaic}$	48.2	195.8	8.4	349
$ET_{G\text{-}Noah}$	45.1	195.2	8.4	9.3
ET_{MODIS}	27	201.8	8	59
ET_{GPS}	47.9	210.4	2.7	298
ET_{GRACE}	56.7	198.8	12.9	0.4

The annual and semi-annual terms of monthly ET variations are defined as $A\sin(2*pi*(t-t_0)/\omega+\varphi)$, where A and φ are the amplitude and phase.

is different from LSM. The energy balance or water balance constraint may result in the difference of ET products from different categories. For the quantitative comparison of different ET products, the annual and semiannual terms of the ET time series are obtained using the common fitting method in Table II. The magnitude of ET products from GLDAS LSMs is larger than that from NLDAS LSMs, and the ET products from MODIS have the smallest magnitude. Different LSMs with different data assimilation [28] result in the different magnitudes of ET products. The magnitude of ET products from MODIS is relatively smaller than others globally. The annual amplitude of GPS is close to the ET products from LSM and a little larger than that from MODIS but smaller than GRACE ET products. The ET variations are mainly controlled by annual terms, and therefore, the semiannual amplitude of ET products is very smaller.

Difference in monthly ET products becomes larger in warm seasons than in cold seasons. The GPS-inferred ET is noisier than other ET products, which is mainly from GPS-inferred TWS. There are also some differences between ET products in mean monthly ET (see Fig. 9). The periodic pattern of radiative energy in a year leads to the seasonal pattern of ET products, which is clearly demonstrated in Fig. 9. The ET estimations from NLDAS VIC, Noah, and MODIS are maximal in July, and the others are maximal in June. The ET estimates from GRACE and GPS are lowest in November, which is different from other ET products in December. The latency may be due to the noise in GPS- and GRACE-inferred TWS.

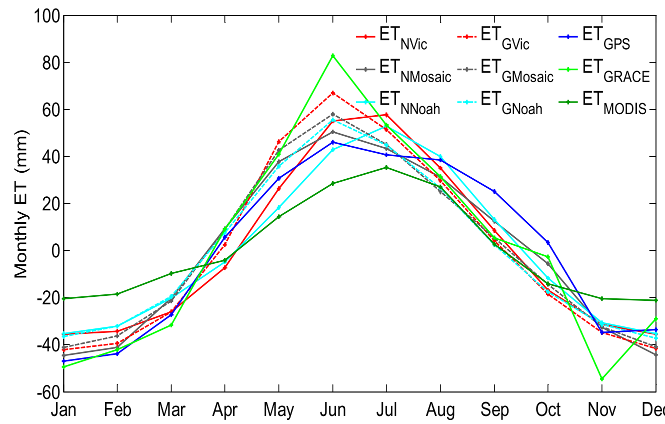

Fig. 9. Mean monthly ET variations from different ET products.

The uncertainties of ET estimation from LSMs, remote sensing, and GRACE have been discussed in [38]. Uncertainties of ET estimated from GPS-inferred TWS depend on the reliability of GPS TWS. The GPS time series consist of signals from different geophysical processes and systematic errors, which may not be removed clearly and affect the GPS-inferred water storage change.

C. Temperature and Soil Moisture Effects

In order to understand the effects of temperature and soil moisture on ET variations, we collected monthly temperature data from PRISM and soil moisture data from 2006 to July 2015. PRISM utilized the data set covering the conterminous United States with station networks of more than 30-year observation data. These data sets are established by implementing some spatial interpolation techniques with climatologic information and terrain characteristics. Here, soil moisture data are obtained from NLDAS-2, which has some improvement when compared with NLDAS-1. With different LSMs such as VIC, Noah, and Mosaic, the soil moisture anomalies have little differences between them; thus, the VIC soil moisture data are taken as examples for comparison. The VIC model has three soil layers, and the estimates from models have been validated by *in situ* observations. The gridded temperature and soil moisture data have spatial resolution of 1/24° and 1/8°, respectively.

The GPS-inferred ET, temperature, and soil moisture anomalies are averaged in MRB to show their coherences in Fig. 10. Pearson's correlation coefficients have been calculated for quantitative comparison. The temperature is highly correlated with ET estimation at a correlation of 0.8, and soil moisture is negatively correlated with ET estimate at a correlation of −0.32. To compare the relative importance of temperature and soil moisture, it is equivalent to distinguish the energy-limited regime or the soil moisture regime on ET variations. In dry regions, the ET variations are strongly controlled by the soil moisture but have little impact on climate change. In wet regions, soil moisture has limited impact on ET variations. The MRB has larger soil moisture across the whole

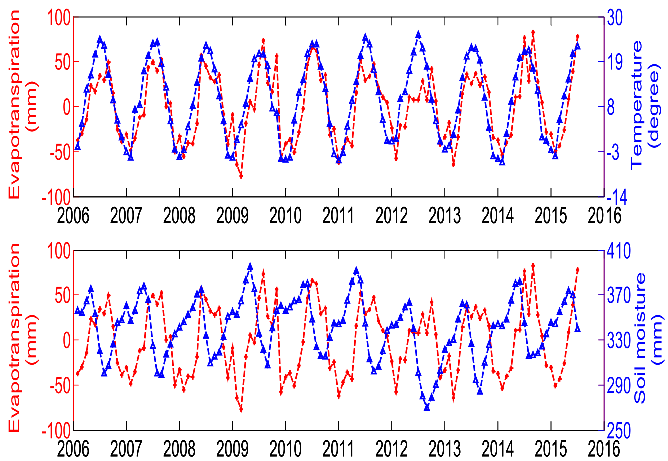

Fig. 10. Correlation of ET variations with (a) surface temperature and (b) soil moisture. All estimates are spatially averaged in MRB from 2006 to 2015.

United States, and the temperature is the key factor to control the ET variations in MRB based on the correlation results.

V. Summary

In this paper, a new GPS tool has been proposed for the first time to estimate the monthly ET variations in MRB. Based on the water balance approach, spatially averaged ET variations from January 2006 to July 2015 in MRB are estimated from GPS-inferred TWS with precipitation from PRISM and runoff from VIC as input data. The monthly GPS ET results are compared with ET products from GRACE, LSM, and MODIS. For the entire study period, the GPS-based ET products have good correlation with other models' ET products. The annual amplitude of GPS-inferred ET is 47.9 mm, close to LSM, larger than MODIS, and smaller than GRACE. The mean monthly ET variations also show good correlation between GPS-based ET and models' ET products. Moreover, the ET products are consistent with the periodic pattern of radiative energy in a year. In addition, the correlation of ET variations is -0.32 with soil moisture and as high as 0.8 with the temperature; thus, the ET variations in MRB are mainly controlled by the temperature. Therefore, GPS-inferred water storage changes have potential to validate and evaluate the models' ET variations at regional scales.

In the future, more precise and denser observations can be obtained from Global Navigation Satellite Systems measurements [40], [41], which may provide us more chances to monitor the hydrological cycle and ET variations in a smaller scale as a new remote sensing.

Acknowledgment

The authors would like to thank JPL's GPS data processing group and the UNAVCO, NSF Plate Boundary Observatory, and NASA MEaSUREs projects for GPS observations and data organization. The GPS data used in this paper are available at ftp://sideshow.jpl.nasa.gov/pub in the directories JPL_GPS_Products and JPL_GPS_Timeseries/repro2011b. The authors would also like to thank those who made GRACE observations available.

References

[1] D. A. Goolsby *et al.*, "Flux and sources of nutrients in the Mississippi-Atchafalaya River basin: Topic 3 Report for the integrated assessment on hypoxia in the Gulf of Mexico," NOAA Coastal Ocean Office, Silver Spring, MA, USA, ser. 17, pp. 1–159, 1999.

[2] M. G. Bosilovich and S. D. Schubert, "Water vapor tracers as diagnostics of the regional hydrologic cycle," *J. Hydrometeorol.*, vol. 3, pp. 149–165, 2002.

[3] W. G. M. Bastiaanssen *et al.*, "SEBAL model with remotely sensed data to improve water resources management under actual field conditions," *ASCE J. Irrigation Drainage Eng.*, vol. 131, no. 1, pp. 85–93, Feb. 2005.

[4] P. J. Webster *et al.*, "Extended-range probabilistic forecasts of Ganges and Brahmaputra floods in Bangladesh," *Bull. Amer. Meteorol. Soc.*, vol. 91, no. 11, pp. 1493–1514, 2010. doi: 10.1175/2010BAMS2911.1.

[5] K. Zhang, J. S. Kimball, R. R. Nemani, and S. W. Running, "A continuous satellite-derived global record of land surface evapotranspiration from 1983 to 2006," *Water Resour. Res.*, vol. 46, no. 9, 2010, Art. no. W09522, doi: 10.1029/2009WR008800.

[6] Q. Z. Mu, M. S. Zhao, and S. W. Running, "Improvements to a MODIS global terrestrial evapotranspiration algorithm," *Remote Sens. Environ.*, vol. 115, no. 8, pp. 1781–1800, Aug. 2011.

[7] P. Nagler *et al.*, "Predicting riparian evapotranspiration from MODIS vegetation indices and meteorological data," *Remote Sens. Environ.*, vol. 94, no. 1, pp. 17–30, Jan. 2005.

[8] J. Overgaard, D. Rosbjereg, and M. Butts, "Land-surface modeling in hydrological perspective—A review," *Biogeosciences*, vol. 3, no. 2, pp. 229–241, May 2006.

[9] L. Jiang and S. Islam, "Estimation of surface evaporation map over southern Great Plains using remote sensing data," *Water Resour. Res.*, vol. 37, no. 2, pp. 329–340, Feb. 2001.

[10] Z. L. Li *et al.*, "A review of current methodologies for regional evapotranspiration estimation from remotely sensed data," *Sensors*, vol. 9, no. 5, pp. 3801–3853, 2009, doi: 10.3390/s90503801.

[11] P. J. F. Yeh, M. Irizarry, and E. A. B. Eltahir, "Hydroclimatology of Illinois: A comparison of monthly evaporation estimates based on atmospheric water balance and soil water balance," *J. Geophys. Res.*, vol. 103, no. D16, pp. 19 823–19 837, Aug. 1998.

[12] B. D. Tapley, S. Bettadpur, M. M. Watkins, and C. Reigber, "The gravity recovery and climate experiment: Mission overview and early results," *Geophys. Res. Lett.*, vol. 31, no. 9, May 2004, Art. no. L09607. doi: 10.1029/2004GL019920.

[13] Y. Fu and J. T. Freymueller, "Seasonal and long-term vertical deformation in the Nepal Himalaya constrained by GPS and GRACE measurements," *J. Geophys. Res.*, vol. 117, no. B3, Mar. 2012, Art. no. B03407. doi: 10.1029/2011JB008925.

[14] S. G. Jin and G. P. Feng, "Large-scale variations of global groundwater from satellite gravimetry and hydrological models, 2002–2012," *Global Planet. Change*, vol. 106, pp. 20–30, Jul. 2013. doi: 10.1016/j.gloplacha.2013.02.008.2013.02.008.

[15] T. H. Syed *et al.*, "Total basin discharge for the Amazon and Mississippi River basins from GRACE and a land–atmosphere water balance," *Geophys. Res. Lett.*, vol. 32, no. 24, Dec. 2005, Art. no. L24404. doi: 10.1029/2005GL024851.

[16] G. Ramillien *et al.*, "Time variations of the regional evapotranspiration rate from gravity recovery and climate experiment (GRACE) satellite gravimetry," *Water Resour. Res.*, vol. 42, no. 10, Oct. 2006, Art. no. W10403. doi: 10.1029/2005WR004331.

[17] M. Rodell *et al.*, "Basin scale estimates of evapotranspiration using GRACE and other observations," *Geophys. Res. Lett.*, vol. 31, no. 20, Oct. 2004, Art. no. L20504. doi: 10.1029/2004GL020873.

[18] S. G. Jin and X. G. Zhang, "A Tikhonov regularization method to estimate Earth's oblateness variations from global GPS observations," *J. Geodyn.*, vol. 79, pp. 23–29, Sep. 2014. doi: 10.1016/j.jog.2014.04.011.

[19] J. Wahr *et al.*, "The use of GPS horizontals for loading studies, with applications to Northern California and Southeast Greenland," *J. Geophys. Res. Solid Earth*, vol. 118, no. 4, pp. 1795–1806, Apr. 2013. doi: 10.1002/jgrb.50104.

[20] D. F. Argus, Y. Fu, and F. W. Landerer, "Seasonal variation in total water storage in California inferred from GPS observations of vertical land motion," *Geophys. Res. Lett.*, vol. 41, no.6, pp. 1971–1980, Mar. 2014. doi: 10.1002/2014GL059570.

[21] Y. Fu, D. F. Argus, and F. W. Landerer, "GPS as an independent measurement to estimate terrestrial water storage variations in Washington and Oregon," *J. Geophys. Res. Solid Earth*, vol. 120, no. 1, Jan. 2015. doi: 10.1002/2014JB011415.

[22] P. Elósegui, J. L. Davis, J. X. Mitrovica, R. A. Bennett, and B. P. Wernicke, "Crustal loading near Great Salt Lake, Utah," *Geophys. Res. Lett.*, vol. 30, no. 3, p. 1111, Feb. 2003. doi: 10.1029/2002GL016579.

[23] M. Bevis *et al.*, "Seasonal fluctuations in the mass of the Amazon River system and Earth's elastic response," *Geophys. Res. Lett.*, vol. 32, no. 16, 2005, Art. no. L16308. doi: 10.1029/2005GL023491.

[24] T. van Dam, NCEP Derived 6 Hourly, Global Surface Displacements at 2.5 × 2.5 Degree Spacing, 2010. [Online]. Available: http://geophy.uni.lu/ncep-loading.html

[25] C. Daly *et al.*, "Physiographically sensitive mapping of climatological temperature and precipitation across the conterminous united states," *Int. J. Climatol.*, vol. 28, no. 15, pp. 2031–2064, Dec. 2008.

[26] C. Daly, R. P. Neilson, and D. L. Phillips, "A statistical-topographic model for mapping climatological precipitation over mountainous terrain," *J. Appl. Meteorol.*, vol. 33, pp. 140–158, Feb. 1994.

[27] M. Di Luzio, G. L. Johnson, C. Daly, J. K. Eischeid, and J. G. Arnold, "Constructing retrospective gridded daily precipitation and temperature datasets for the conterminous United States," *J. Appl. Meteorol. Climatol.*, vol. 47: 475–497, Feb. 2008.

[28] K. E. Mitchell *et al.*, "The multi-institution North American Land Data Assimilation System (NLDAS): Utilizing multiple GCIP products and partners in a continental distributed hydrological modeling system," *J. Geophys. Res.*, vol. 109, no. D7, Apr. 2004, Art. no. D07S90. doi: 10.1029/2003JD003823.

[29] T. J. Troy, E. F. Wood, and J. Sheffield, "An efficient calibration method for continental-scale land surface modeling," *Water Resour. Res.*, vol. 44, no. 9, Sep. 2008, Art. no. W09411. doi: 10.1029/2007WR006513.

[30] W. E. Farrell, "Deformation of the Earth by surface loads," *Rev. Geophys.*, vol. 10, no. 3, pp. 761–797, Aug. 1972. doi: 10.1029/RG010i003p00761.

[31] T. H. Syed, P. J. Webster, and J. S. Famiglietti, "Assessing variability of evapotranspiration over the Ganga River basin using water balance computations," *Water Resour. Res.*, vol. 50, no. 3, pp. 2551–2565, Mar. 2014. doi: 10.1002/2013WR013518.

[32] S. C. Swenson and J. Wahr, "Post-processing removal of correlated errors in GRACE data," *Geophys. Res. Lett.*, vol. 33, no. 8, Apr. 2006, Art. no. L08402. doi: 10.1029/2005GL025285.

[33] M. Cheng and B. D. Tapley, "Variations in the Earth's oblateness during the past 28 years," *J. Geophys. Res.*, vol. 109, no. B9, Sep. 2004, Art. no. B09402. doi: 10.1029/2004JB003028.

[34] F. W. Landerer and S. C. Swenson, "Accuracy of scaled GRACE terrestrial water storage estimates," *Water Resour. Res.*, vol. 48, no. 4, Apr. 2012, Art. no. W04531. doi: 10.1029/2011WR011453.

[35] S. Swenson and J. Wahr, "Methods for inferring regional surface mass anomalies from gravity recovery and climate experiment (GRACE) measurements of time-variable gravity," *J. Geophys. Res.*, vol. 107, no. B9, p. 2193, Sep. 2002. doi: 10.1029/2001JB000576.

[36] J. Huang, M. Véronneau, and A. Mainville, "Assessment of systematic errors in the surface gravity anomalies over North America using the GRACE gravity model," *Geophys. J. Int.*, vol. 175, no. 1, pp. 46–54, Oct. 2008. doi: 10.1111/j.1365-246X.2008.03924.x.

[37] J. Ray, Z. Altamimi, X. Collieux, and T. van Dam, "Anomalous harmonics in the spectra of GPS position estimates," *GPS Solut.*, vol. 12, pp. 55–64, 2008. doi: 10.1007/s10291-007-0067-7.

[38] D. Long, L. Longuevergne, and B. R. Scanlon, "Uncertainty in evapotranspiration from land surface modeling, remote sensing, and GRACE satellites," *Water Resour. Res.*, vol. 50, no. 2, pp. 1131–1151, Feb. 2014. doi: 10.1002/2013WR014581.

[39] M. Rodell, E. B. McWilliams, J. S. Famiglietti, H. K. Beaudoing, and J. Nigro, "Estimating evapotranspiration using and observation based terrestrial water budget," *Hydrol. Process.*, vol. 25, no. 26, pp. 4082–4092, Dec. 2011. doi: 10.1002/hyp.8369.

[40] S. G. Jin, G. P. Feng, and S. Gleason, Remote sensing using GNSS signals: Current status and future directions," *Adv. Space Res.*, vol. 47, no. 10, pp. 1645–1653, May 2011. doi: 10.1016/j.asr.2011.01.036.

[41] S. G. Jin, E. Cardellach, and F. Xie, *GNSS Remote Sensing: Theory, Methods and Applications*. Dordrecht, The Netherlands: Springer-Verlag, 2014.

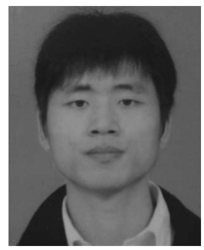

Tengyu Zhang was born in Jiangxi, China, in October 1989. He received the B.Sc. degree from Wuhan University, Wuhan, China, in 2011. He is currently working toward the Ph.D. degree in the Shanghai Astronomical Observatory, Chinese Academy of Sciences, Shanghai, China.

He is also with the University of Chinese Academy of Sciences, Beijing, China. His research interests include satellite navigation, satellite gravimetry, space geodesy, and geodynamics.

Shuanggen Jin (M'05) was born in Anhui, China, in September 1974. He received the B.Sc. degree in geodesy from Wuhan University, Wuhan, China, in 1999 and the Ph.D. degree in geodesy from the University of Chinese Academy of Sciences, Beijing, China, in 2003.

He is currently a Professor with Shanghai Astronomical Observatory, Chinese Academy of Sciences, Shanghai, China and also with the Department of Geomatics Engineering, Bülent Ecevit University, Zonguldak, Turkey. His main research areas include satellite navigation, remote sensing, satellite gravimetry, space/planetary exploration, and dynamics. He has more than 300 papers in the *Journal of Geophysical Research*, IEEE, *Earth and Planetary Science Letters*, *Geophysical Journal International*, *Icarus*, *Journal of Geodynanmics*, etc.; eight patents/software copyrights; and seven books/monographs with more than 1600 citations.

Prof. Jin is the President of the International Association of Planetary Sciences (2013–2017) and the International Association of CPGPS (2016–2017); the Chair of the IUGG Union Commission on Planetary Sciences (2015–2019); the Vice-President of the IAG Commission 2 (2015–2019); the Editor-in-Chief of the *International Journal of Geosciences* (since 2010); an Associate Editor of the IEEE TRANSACTIONS ON GEOSCIENCE AND REMOTE SENSING (since 2014), the *Journal of Navigation* (since 2014), and *Advances in Space Research* (since 2013); and an Editorial Board Member of the *Journal of Geodynamics* (since 2014) and *Planetary and Space Science* (since 2014). He was the recipient of four Provincial Awards of Second Prize, 100-Talent Program of CAS (2010), Fellow of IAG (2011), Fu Chengyi Youth Science and Technology Award (2012), and Xia Jianbai Award of Geomatics (2014), etc.